photochem

MDPI

Article

Modeling the Unimolecular Decay Dynamics of the Fluorinated Criegee Intermediate, CF_3CHOO

Lily M. Guidry [1,†,‡], Courtney A. Poirier [1,2,‡], Jordyn M. Ratliff [1,†], Ernest Antwi [2], Barbara Marchetti [1,*] and Tolga N. V. Karsili [1,*]

[1] Department of Chemistry, University of Louisiana at Lafayette, Lafayette, LA 70504, USA; lily.guidry1@louisiana.edu (L.M.G.); courtney.poirier1@louisiana.edu (C.A.P.); jordyn.ratliff1@louisiana.edu (J.M.R.)

[2] Regional Application Center, NASA/University of Louisiana at Lafayette, Lafayette, LA 70506, USA; ernest.antwi1@louisiana.edu

* Correspondence: barbara.marchetti1@louisiana.edu (B.M.); tolga.karsili@louisiana.edu (T.N.V.K.)

† These authors contributed as undergraduate research students.

‡ These authors contributed equally to this work.

Abstract: When volatile alkenes are emitted into the atmosphere, they are rapidly removed by oxidizing agents such as hydroxyl radicals and ozone. The latter reaction is termed ozonolysis and is an important source of Criegee intermediates (CIs), i.e., carbonyl oxides, that are implicated in enhancing the oxidizing capacity of the troposphere. These CIs aid in the formation of lower volatility compounds that typically condense to form secondary organic aerosols. CIs have attracted vast attention over the past two decades. Despite this, the effect of their substitution on the ground and excited state chemistries of CIs is not well studied. Here, we extend our knowledge obtained from prior studies on CIs by CF_3 substitution. The resulting CF_3CHOO molecule is a CI that can be formed from the ozonolysis of hydrofluoroolefins (HFOs). Our results show that the ground state unimolecular decay should be less reactive and thus more persistent in the atmosphere than the non-fluorinated analog. The excited state dynamics, however, are predicted to occur on an ultrafast timescale. The results are discussed in the context of the ways in which our study could advance synthetic chemistry, as well as processes relevant to the atmosphere.

Keywords: Hydrofluoroolefin refrigerants; atmospheric chemistry; atmospheric photochemistry

check for updates

Citation: Guidry, L.M.; Poirier, C.A.; Ratliff, J.M.; Antwi, E.; Marchetti, B.; Karsili, T.N.V. Modeling the Unimolecular Decay Dynamics of the Fluorinated Criegee Intermediate, CF_3CHOO. *Photochem* **2023**, *3*, 327–335. https://doi.org/10.3390/photochem3030020

Academic Editor: Rui Fausto

Received: 1 June 2023
Revised: 1 July 2023
Accepted: 11 July 2023
Published: 14 July 2023

1. Introduction

Hydrofluorooelfins (HFOs) are unsaturated organofluorides that are used in modern-day refrigerants [1–3]. These fourth-generation refrigerants are of particular interest, as they have been manufactured to replace harmful chlorofluorocarbons (CFCs), hydrochlorofluorocarbons (HCFCs), and hydrofluorocarbons (HFCs). HFOs are preferred over CFCs, HCFCs, and HFCs due to their very low global warming and zero ozone depletion potentials [4,5]. This is a consequence of their short lifetimes in the troposphere, as they undergo oxidation via OH and Cl radicals, as well as with O_3 [6,7].

While much is known about HFO molecules themselves, little is known about the (photo)reactivities of their oxidation products. In the atmosphere, HFOs may react with ozone through ozonolysis across an olefinic C=C bond. Figure 1 provides an example of such a reaction with a common HFO refrigerant, 3,3,3-trifluoro-1-propene (HFO-1243zf), wherein ozonolysis occurs via a [3+2]-cycloaddition of the ozone across the C=C double bond of HFO-1243zf, resulting in the formation of a primary ozonide (POZ). Since the [3+2]-cycloaddition reaction is highly exothermic, the POZ that is formed is highly internally excited, decaying faster than the timescale for collisional energy relaxation that would otherwise form a stabilized POZ. Its unimolecular decay occurs via the cleavage of the five-membered ring center C-C and one of the two O-O bonds, yielding two distinct

products: H_2COO + CF_3CHO or CF_3CHOO + H_2CO. These H_2COO and CF_3CHOO products are known as Criegee intermediates (CIs), which are recognized for enhancing the oxidating capacity of the atmosphere and are implicated in secondary organic aerosol formation [8–11].

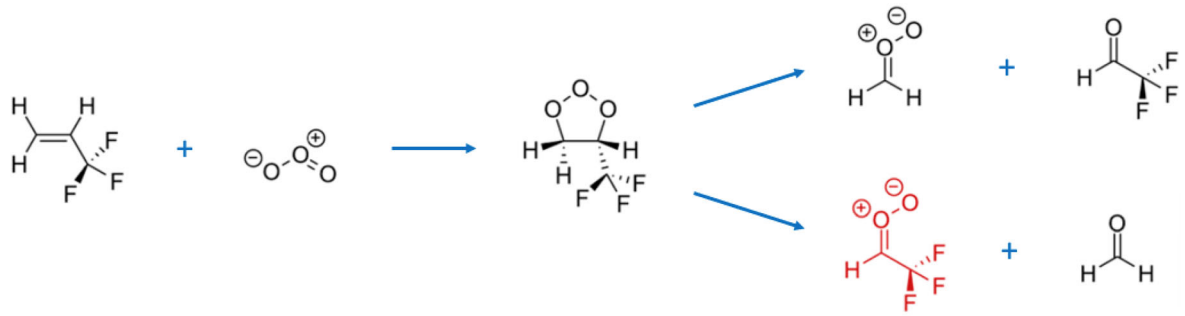

Figure 1. Schematic reaction path displaying the ozonolysis of the HFO-1243zf refrigerant. The molecule of interest in this study is shown in red (trifluoroacetaldehyde oxide—CF_3CHOO).

Non-fluorine-containing CIs (such as H_2COO) are formed in the atmosphere when volatile alkenes undergo ozonolysis. The simplest alkyl-substituted CI is acetaldehyde oxide (CH_3CHOO), which is formed from the ozonolysis of molecules such as propene. It may be formed in the *syn*- or *anti*-conformer. CH_3CHOO can undergo unimolecular decay via intramolecular hydrogen-atom transfer, forming a vinyl hydroperoxide (VHP), which subsequently decays to form vinoxy and OH radicals [10,12–14]. While this process is favored in *syn*-CH_3CHOO, *anti*-CH_3CHOO unimolecular decay is dominated by the formation of methyl dioxirane or acetic acid ($CH_3C(O)OH$) via isomerization, which decays to form CH_3CO + OH, CH_4 + CO_2, and CH_3OH + CO. CH_3CHOO, especially in the *anti*-conformation, can also undergo bimolecular chemistry with trace tropospheric gases such as H_2O, SO_2, and HCOOH [15]. The photochemical properties of CH_3CHOO are also worth discussing [16,17]. Using UV action spectroscopy and velocity map imaging on jet-cooled CH_3CHOO, Lester and co-workers showed through their studies that the photodissociation of this molecule led to the formation of CH_3CHO + O products after excitation at $\lambda < 350$ nm. This dissociation resulted in two spin-allowed channels forming CH_3CHO (S_0) + O (^1D) and CH_3CHO (T_1) + O (^3P) products, with the latter becoming energetically accessible at $\lambda \leq 324$ nm. Using trajectory surface hopping (TSH), where the energies, gradients, and non-adiabatic couplings were computed "on-the-fly" using MS-CASPT2, we previously assessed the dynamics of CH_3CHOO following excitation to the S_2 state. O-O bond dissociation was observed to be the dominant decay channel, forming CH_3CHO (S_0) + O (^1D) products [16].

In this manuscript, we explore the effects of fluorination on the ground state unimolecular decay and photodissociation dynamics of *syn*- and *anti*-CF_3CHOO.

2. Methodology

The ground state minimum energy geometries of CH_3CHOO and CF_3CHOO, along with their respective dioxirane products and transition states, were optimized at the m06-2x/aug-cc-pVTZ level of theory using the Gaussian computational package [18]. Using the CCSD(T)-F12/cc-pVTZ-F12 level of theory, single-point energy calculations were computed on the optimized structures, which allowed us to obtain more accurate energies. These latter calculations were carried out in Molpro [19,20]. This combination of m06-2x/aug-cc-pVTZ//CCSD(T)-F12 was successfully applied to develop a structure–activity relationship of the unimolecular decay kinetics of substituted Criegee intermediates [21,22].

The fate of the excited states of CF_3CHOO was modeled using TSH and static electronic structure calculations. TSH simulations were carried out using the Newton-X computational package [23,24]. Initial conditions were acquired using a Wigner distribution based on the B2PLYP-D3/cc-pVTZ equilibrium geometry of *syn*- and *anti*- CF_3CHOO and their

respective harmonic normal mode wavenumbers. As shown in prior findings, this level of theory performs well in obtaining the geometries and normal modes of CIs and their associated reaction profiles [25–32]. In TSH, the nuclei were propagated by integrating Newton's equation using the velocity Verlet method, while the electronic coordinates were treated quantum-mechanically by numerically solving the time-dependent Schrodinger equation using Butcher's fifth-order Runge–Kutta method in steps of 0.025 fs [33]. Trajectories were initiated on the bright S_2 state. Energies, forces, and non-adiabatic coupling matrix elements were computed on-the-fly, using the single-state, single-reference complete active space second-order perturbation theory (SS-SR-CASPT2) method along with the cc-pVDZ basis set. These energies/forces were computed via the BAGEL interface to Newton-X [34,35]. SS-SR-CASPT2 not only produced energies and analytical gradients at the MS-CASPT2 quality at a reduced computational cost, but also performed well near electronic state degeneracies. SS-SR-CASPT2 calculations were based on a state-averaged complete active space self-consistent field (CASSCF) method reference wavefunction and an active space composed of 10 electrons in 8 orbitals. Additional potential energy profiles were computed in order to assess the excited state reaction paths along the O-O stretch coordinate. These were computed using Molpro at the CASPT2/aug-cc-pVTZ level of theory and using the same 10/8 active space as the previously mentioned TSH simulations. Due to the highly multi-reference nature of the excited-state dynamics of the Criegee intermediate, these methods were required for modeling the excited states of our present systems. Our previous studies have highlighted the success of SS-SR-CASPT2 in assessing the excited state dynamics and energy profiles of Criegee intermediates [29].

3. Results and Discussion

Figure 2 displays the ground state minimum energy geometry of the *syn*- and *anti*-conformers of CF_3CHOO. These conformers are distinguishable by the orientation of the terminal oxygen atom relative to the CF_3 group. *Anti*-CF_3CHOO is the most stable conformer and is predicted to be ca. 0.6 kcal mol^{-1} more stable than *syn*-CF_3CHOO). This observation is in contrast to CH_3CHOO [12], which showed a preference for forming *syn*-conformers due to the weak intramolecular hydrogen–bonding interaction between the CH_3-centered H-atoms and the terminal oxygen atom. Since this interaction does not exist in *syn*-CF_3CHOO, *anti*-CF_3CHOO shows less steric hindrance (cf. *syn*-CF_3CHOO). The equivalent energy difference between *syn*- and *anti*-CH_3CHOO was ca. 3.7 kcal mol^{-1}, with a barrier height of ca. 38 kcal mol^{-1}.

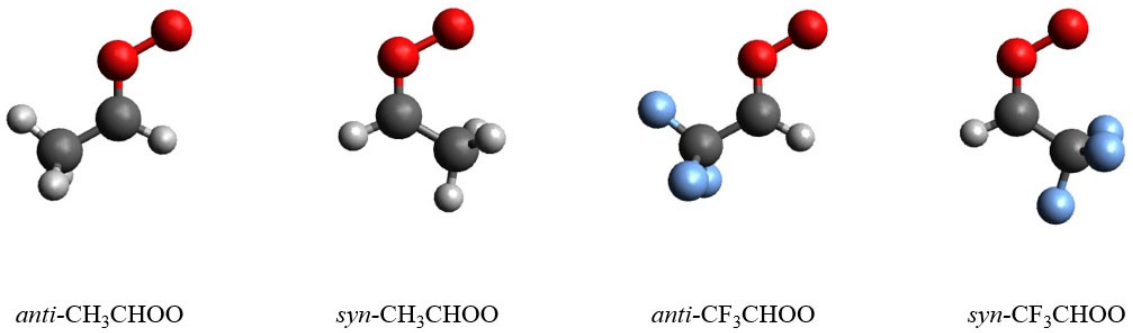

Figure 2. Minimum energy structures of *anti*- and *syn*-H_3CHOO and *anti*- and *syn*-CF_3CHOO.

Guided by previous studies on the ozonolysis of CIs, CF_3CHOO is expected to undergo bimolecular chemistry with trace gases in the atmosphere or unimolecular decay either thermally or after UV excitation. Here, we focused on the latter two unimolecular decay paths. Figure 3a,c displays the energy profiles that are associated with the two most prominent unimolecular decay paths of CH_3CHOO—i.e., isomerization to form vinyl hydroperoxide (VHP) or methyldioxirane. VHP formation involves 1,4-hydrogen-atom migration and is the dominant unimolecular decay path for the more stable (*syn*) conformer of CH_3CHOO, and is predicted to contain a transition state barrier of ca. 18 kcal mol^{-1}—which

is in excellent agreement with prior high-level quantum chemical studies [36]. The equivalent isomerization in CF_3CHOO involves a 1,4-fluorine atom migration (Figure 3d). As expected, the energy profile associated with the F-atom migration contained a transition state barrier that was ca. 60 kcal mol^{-1} higher than the equivalent H-atom migration in *syn*-CH_3CHOO—manifesting from an unfavorable C-F bond fission and an unfavorable OF bond formation. In contrast, the cyclization of CF_3CHOO to form dioxirane contained a transition state barrier that was comparable to that of CH_3CHOO (Figure 3a,b). We, therefore, expect cyclization to be the only competitive thermal removal process in CF_3CHOO, which is expected to proceed with a low rate constant. Under low humidity conditions, we expect CF_3CHOO to be long-lived when compared to the typical sub-second atmospheric lifetime of CIs. As such, it could absorb UV radiation and become photo-excited.

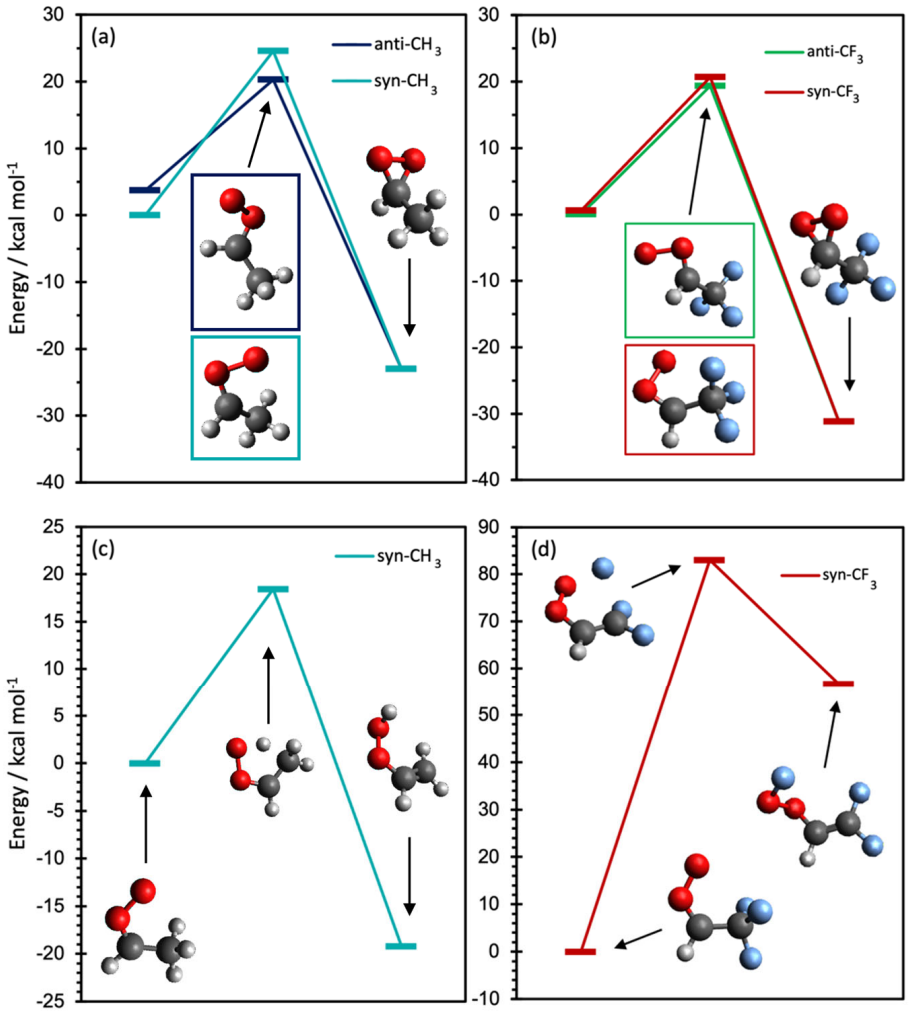

Figure 3. Reaction energy profiles associated with the unimolecular decay paths available to CH_3CHOO and CF_3CHOO; dioxirane formation in (**a**) CH_3CHOO and (**b**) CF_3CHOO, (**c**) 1,4-H migration in *syn*-CH_3CHOO and (**d**) F-migration in *syn*-CF_3CHOO. Panels (**a**,**b**) represent the cyclization to form dioxirane products, while (**c**,**d**) represent the energy profile associated with intramolecular hydrogen or fluorine atom transfer, respectively.

Figure 4 presents the orbitals and orbital promotions that are associated with electronic excitation to the S_1 and S_2 states. As with other CIs, excitation to the S_1 state arises via a $\pi^* \leftarrow n$ orbital promotion and contains zero oscillator strength. In contrast, excitation to the S_2 state involves a $\pi^* \leftarrow \pi$ electron promotion, which is the transition that dominates the near-UV absorption. This aligns with previous observations of CIs [17].

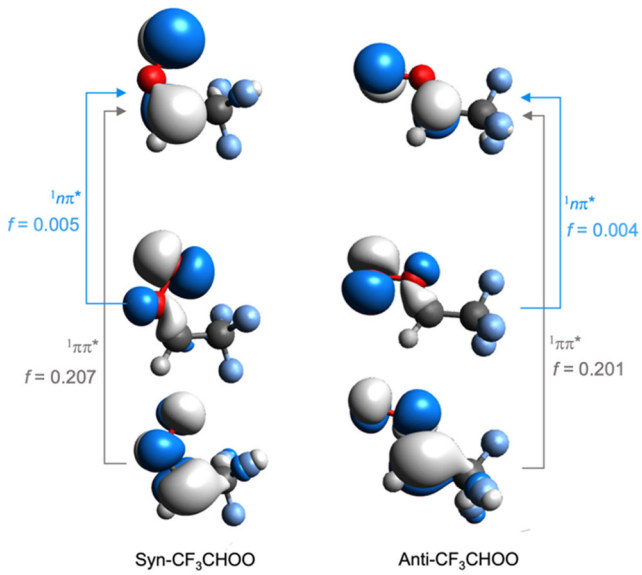

Figure 4. Orbitals and orbital promotions associated with excitation to the lowest two single excited electronic states of *syn*- and *anti*-CF_3CHOO.

Following excitation to the bright S_2 state, our TSH simulations (Figure 5) revealed fast deactivation of the S_2 state within 40 fs. An analysis of the TSH simulations reveals that both the *syn*- and *anti*-conformers dominantly undergo O-O bond elongation within 40 fs, leading to the formation of CF_3CHO + O products with a unity quantum yield. In the higher energy *syn*-conformer (Figure 5b), prompt internal conversion at early time revealed partitioning of the population to all seven electronic states. By contrast, only the S_0, S_1, S_2, S_3, and S_4 states are populated in the *anti*-conformer—i.e., the lower energy conformer.

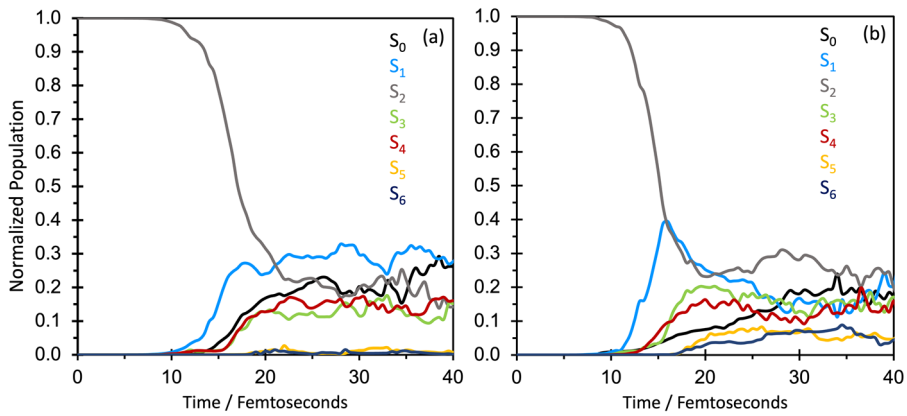

Figure 5. The time evolution of the populations for excitation to the S_2 state of (**a**) *anti*-CF_3CHOO and (**b**) *syn*-CF_3CHOO.

As the CASPT2 PE profiles along the O-O elongation coordinate (Figure 6) reveal, the S_0, S_1, S_2, S_3 and S_4 states correlate with the lower energy asymptote, corresponding to $O(^1D)$ + $CF_3CHO(S_0)$ products, while the S_5 and S_6 states correlate with the second asymptote, which corresponds to the $O(^3P)$ + $CF_3CHO(T_1)$ product asymptote. The electronic state character of the S_0-S_6 states was the same as those reported in our earlier work [37], which are briefly outlined in the following text. In the former cluster of states, S_0 involves an intuitive long-range attractive interaction that arises via the interaction between the CF_3CHO-centered O-2p lone pair and the vacant 2p orbital on $O(^1D)$. At long R_{OO}, this same 2p orbital is either singly or doubly occupied in the S_1-S_4 state configurations and manifests in the long-range repulsive interaction that is observed for these states in Figure 6. The S_5 and S_6 states contain a long-range attractive interaction, which can be understood by

considering that the T_1 state of formaldehyde is of the nπ* character, with an odd electron in the oxygen-centered 2p lone pair. This odd electron forms a bonding pair with one of the two odd electrons in the 2p orbital of the O(^{3}P) atom. This agrees with previous observations of CI's photochemistry [17]. As noted in the above description, in the *anti*-conformer, a negligible portion of the starting population partitions to the higher energy S_5 and S_6 states, manifesting in a negligible yield of O(^{3}P) + $CF_3CHO(T_1)$ products. By contrast, for the *syn*-conformer, ca. 15% of the initially excited population partitions across the S_5 and S_6 states, giving ca. 15% yield of O(^{3}P) + $CF_3CHO(T_1)$ products within 40 fs. This latter observation is in line with a previous observation of the simplest CI, CH_2OO, which returned an equally low fraction of the overall population into O(^{3}P) + $CH_2O(T_1)$ products [29]. This observation is striking and may be plausibly explained by the weaker interaction between S_3/S_4 and S_5/S_6 states or by a perturbation caused by the CF_3 moiety on the O atom leaving group.

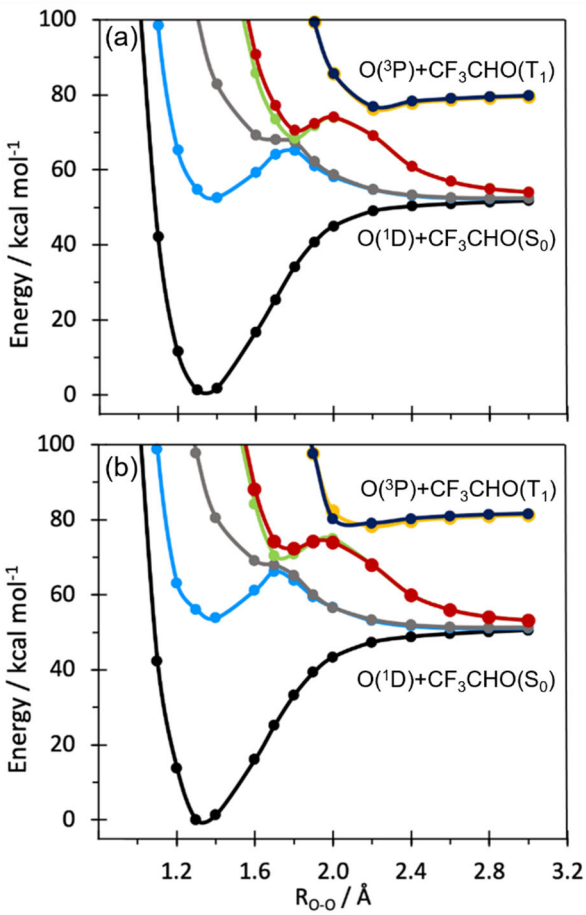

Figure 6. Adiabatic potential energy profiles along the O-O stretch coordinate for the lowest seven singlet states of (**a**) *anti*-CF_3CHOO and (**b**) *syn*-CF_3CHOO.

The dominant nuclear motions associated with these internal conversions can be understood by assessing the PE profiles in Figure 6, which show two avoided crossings. These avoided crossings will develop into conical intersections when motions along orthogonal motions are considered. The first avoided crossing is at R_{OO}~1.7 Å, which involves a four-state intersection involving the S_1, S_2, S_3, and S_4 states. The early time internal conversation observed in the TSH results arises via an internal conversion at these crossing points. A second avoided crossing can be observed at R_{OO}~2.2 Å between the S_3, S_4, S_5, and S_6 states. The ultimate branching into the O(^{1}D) + $CF_3CHO(S_0)$ and O(^{3}P) + $CF_3CHO(T_1)$ products is governed by the rate of internal conversion at this crossing point.

4. Conclusions

In this article, we have reported the details of the ground and excited state unimolecular decay of CF_3CHOO, which can be formed from the ozonolysis of commonly used HFOs. Unlike CH_3CHOO, the two *syn*- and *anti*-conformers of CF_3CHOO are energetically close, manifesting from the absence of hydrogen bonding that is present in *syn*-CH_3CHOO. Our results show that the unimolecular decay of CF_3CHOO is expected to follow an analogous cyclization to form dioxirane products but with a slightly lower energy barrier. Unlike CH_3CHOO, however, *syn*-CF_3CHOO does not have an analogous hydrogen atom transfer that forms a vinyl hydroperoxide. As demonstrated in our results above, the analogous fluorine atom transfer is, as expected, unfavorable. As with other CIs, the electronic absorption of CF_3CHOO is dominated by the S_2 state, which arises via a $\pi^* \leftarrow \pi$ transition. Excitation to this state leads to prompt O-O bond fission, forming $O(^1D)$ products in both *syn*-CF_3CHOO and *anti*-CF_3CHOO. Unlike CH_2OO, the $O(^3P)$ channel was unobserved in *anti*-CF_3CHOO.

These results shed light on the expected ground and excited state chemistry of an HFO-derived CI. When HFO refrigerants are emitted into the atmosphere, their primary removal is via a reaction with OH radicals; however, reaction with O_3 is relevant in ozone-rich environments. Our studies are also relevant to the synthetic chemistry community, since the results highlight the effect of a CF_3 substitution on the ground and excited state dynamics of a substituted CI. When compared to our previous studies on CFHOO, the effect of CF_3 substitution was much less dramatic than F substitution, which is most likely due to the weaker π-perturbing effect of CF_3 versus F.

Our future studies aim to focus on the bimolecular chemistry of CF_3CHOO and how its chemistry compares to CH_3CHOO. Since some HFOs contain a chlorine substituent, we would also be excited to explore the effect of chlorination on the ground and the excited state chemistry of CIs.

Author Contributions: Conceptualization, B.M. and T.N.V.K.; methodology, L.M.G., C.A.P., J.M.R. and E.A.; validation, L.M.G., C.A.P., J.M.R., E.A., T.N.V.K. and B.M.; formal analysis, L.M.G., C.A.P., J.M.R., E.A., T.N.V.K. and B.M.; investigation, L.M.G., C.A.P., J.M.R. and E.A.; resources, T.N.V.K.; data curation, L.M.G., C.A.P., J.M.R. and E.A.; writing—original draft preparation, L.M.G. and C.A.P.; writing—review and editing, T.N.V.K. and B.M.; supervision, T.N.V.K. and B.M.; funding acquisition, T.N.V.K. All authors have read and agreed to the published version of the manuscript.

Funding: This research was funded by National Science Foundation, under grant no. 2003422.

Data Availability Statement: The data underpinning this study will be made available upon reasonable request by contacting the corresponding authors.

Acknowledgments: The work reported in this article is supported by the National Science Foundation, under grant no. 2003422. C.A.P. thanks the National Science Foundation (2120015) for the award of a research assistantship. Portions of this research were conducted with high performance computational resources provided by the Louisiana Optical Network Infrastructure.

Conflicts of Interest: The authors declare no conflict of interest.

References

1. Mateu-Royo, C.; Navarro-Esbrí, J.; Mota-Babiloni, A.; Amat-Albuixech, M.; Molés, F. Thermodynamic analysis of low GWP alternatives to HFC-245fa in high-temperature heat pumps: HCFO-1224yd(Z), HCFO-1233zd(E) and HFO-1336mzz(Z). *Appl. Therm. Eng.* **2019**, *152*, 762–777. [CrossRef]
2. Molés, F.; Navarro-Esbrí, J.; Peris, B.; Mota-Babiloni, A.; Barragán-Cervera, Á.; Kontomaris, K. Thermo-economic evaluation of low global warming potential alternatives to HFC-245fa in Organic Rankine Cycles. *Energy Procedia* **2017**, *142*, 1199–1205. [CrossRef]
3. Navarro-Esbrí, J.; Molés, F.; Peris, B.; Mota-Babiloni, A.; Kontomaris, K. Experimental study of an Organic Rankine Cycle with HFO-1336mzz-Z as a low global warming potential working fluid for micro-scale low temperature applications. *Energy* **2017**, *133*, 79–89. [CrossRef]

4. Molés, F.; Navarro-Esbrí, J.; Peris, B.; Mota-Babiloni, A.; Barragán-Cervera, Á.; Kontomaris, K. Low GWP alternatives to HFC-245fa in Organic Rankine Cycles for low temperature heat recovery: HCFO-1233zd-E and HFO-1336mzz-Z. *Appl. Therm. Eng.* **2014**, *71*, 204–212. [CrossRef]
5. Fouad, W.A.; Vega, L.F. Next generation of low global warming potential refrigerants: Thermodynamic properties molecular modeling. *AIChE J.* **2018**, *64*, 250–262. [CrossRef]
6. Rivela, C.B.; Tovar, C.M.; Teruel, M.A.; Barnes, I.; Wiesen, P.; Blanco, M.B. CFCs replacements: Reactivity and atmospheric lifetimes of a series of Hydrofluoroolefins towards OH radicals and Cl atoms. *Chem. Phys. Lett.* **2019**, *714*, 190–196. [CrossRef]
7. Rao, P.K.; Gejji, S.P. Atmospheric degradation of HCFO-1233zd(E) initiated by OH radical, Cl atom and O_3 molecule: Kinetics, reaction mechanisms and implications. *J. Fluor. Chem.* **2018**, *211*, 180–193. [CrossRef]
8. Donahue, N.M.; Drozd, G.T.; Epstein, S.A.; Presto, A.A.; Kroll, J.H. Adventures in ozoneland: Down the rabbit-hole. *Phys. Chem. Chem. Phys.* **2011**, *13*, 10848–10857. [CrossRef]
9. Osborn, D.L.; Taatjes, C.A. The physical chemistry of Criegee intermediates in the Gas Phase. *Int. Rev. Phys. Chem.* **2015**, *34*, 309–360. [CrossRef]
10. Lester, M.I.; Klippenstein, S.J. Unimolecular Decay of Criegee Intermediates to OH Radical Products: Prompt and Thermal Decay Processes. *Acc. Chem. Res.* **2018**, *51*, 978–985. [CrossRef]
11. Chhantyal-Pun, R.; Khan, M.A.H.; Taatjes, C.A.; Percival, C.J.; Orr-Ewing, A.J.; Shallcross, D.E. Criegee intermediates: Production, detection and reactivity. *Int. Rev. Phys. Chem.* **2020**, *39*, 383–422. [CrossRef]
12. Liu, F.; Beames, J.M.; Petit, A.S.; McCoy, A.B.; Lester, M.I. Infrared-driven unimolecular reaction of CH_3CHOO Criegee intermediates to OH radical products. *Science* **2014**, *345*, 1596–1598. [CrossRef] [PubMed]
13. Fang, Y.; Liu, F.; Barber, V.P.; Klippenstein, S.J.; McCoy, A.B.; Lester, M.I. Deep tunneling in the unimolecular decay of CH_3CHOO Criegee intermediates to OH radical products. *J. Chem. Phys.* **2016**, *145*, 234308. [CrossRef] [PubMed]
14. Barber, V.P.; Pandit, S.; Esposito, V.J.; McCoy, A.B.; Lester, M.I. CH Stretch Activation of CH_3CHOO: Deep Tunneling to Hydroxyl Radical Products. *J. Phys. Chem. A* **2019**, *123*, 2559–2569. [CrossRef]
15. Newland, M.J.; Rickard, A.R.; Sherwen, T.; Evans, M.J.; Vereecken, L.; Muñoz, A.; Ródenas, M.; Bloss, W.J. The atmospheric impacts of monoterpene ozonolysis on global stabilised Criegee intermediate budgets and SO_2 oxidation: Experiment, theory and modelling. *Atmos. Chem. Phys.* **2018**, *18*, 6095–6120. [CrossRef]
16. Li, H.; Fang, Y.; Kidwell, N.M.; Beames, J.M.; Lester, M.I. UV Photodissociation Dynamics of the CH_3CHOO Criegee Intermediate: Action Spectroscopy and Velocity Map Imaging of O-Atom Products. *J. Phys. Chem. A* **2015**, *119*, 8328–8337. [CrossRef] [PubMed]
17. Karsili, T.N.V.; Marchetti, B.; Lester, M.I.; Ashfold, M.N.R. Electronic Absorption Spectroscopy and Photochemistry of Criegee Intermediates. *Photochem. Photobiol.* **2022**, *99*, 4–18. [CrossRef]
18. Frisch, M.J.; Trucks, G.W.; Schlegel, H.B.; Scuseria, G.E.; Robb, M.A.; Cheeseman, J.R.; Scalmani, G.; Barone, V.; Petersson, G.A.; Nakatsuji, H.; et al. *Gaussian 16, Revision C.01*; Gaussian Inc.: Wallingford, CT, USA, 2016.
19. Werner, H.-J.; Knowles, P.J.; Knizia, G.; Manby, F.R.; Schütz, M. Molpro: A general-purpose quantum chemistry program package. *WIREs Comput. Mol. Sci.* **2012**, *2*, 242–253. [CrossRef]
20. Werner, H.-J.; Knowles, P.J.; Knizia, G.; Manby, F.R.; Schütz, M.; Celani, P.; Györffy, W.; Kats, D.; Korona, T.; Lindh, R.; et al. MOLPRO, Version 2018.1, a Package of Ab Initio Programs. Available online: https://www.molpro.net/ (accessed on 31 May 2023).
21. Vereecken, L.; Novelli, A.; Taraborrelli, D. Unimolecular decay strongly limits the atmospheric impact of Criegee intermediates. *Phys. Chem. Chem. Phys.* **2017**, *19*, 31599–31612. [CrossRef]
22. Vereecken, L.; Novelli, A.; Kiendler-Scharr, A.; Wahner, A. Unimolecular and water reactions of oxygenated and unsaturated Criegee intermediates under atmospheric conditions. *Phys. Chem. Chem. Phys.* **2022**, *24*, 6428–6443. [CrossRef]
23. Barbatti, M.; Granucci, G.; Persico, M.; Ruckenbauer, M.; Vazdar, M.; Eckert-Maksić, M.; Lischka, H. The on-the-fly surface-hopping program system Newton-X: Application to ab initio simulation of the nonadiabatic photodynamics of benchmark systems. *J. Photochem. Photobiol. A Chem.* **2007**, *190*, 228–240. [CrossRef]
24. Barbatti, M.; Ruckenbauer, M.; Plasser, F.; Pittner, J.; Granucci, G.; Persico, M.; Lischka, H. Newton-X: A surface-hopping program for nonadiabatic molecular dynamics. *Wiley Interdiscip. Rev. Comput. Mol. Sci.* **2013**, *4*, 26–33. [CrossRef]
25. Barber, V.P.; Pandit, S.; Green, A.M.; Trongsiriwat, N.; Walsh, P.J.; Klippenstein, S.J.; Lester, M.I. Four-Carbon Criegee Intermediate from Isoprene Ozonolysis: Methyl Vinyl Ketone Oxide Synthesis, Infrared Spectrum, and OH Production. *J. Am. Chem. Soc.* **2018**, *140*, 10866–10880. [CrossRef] [PubMed]
26. Wang, G.; Liu, T.; Caracciolo, A.; Vansco, M.F.; Trongsiriwat, N.; Walsh, P.J.; Marchetti, B.; Karsili, T.N.V.; Lester, M.I. Photodissociation dynamics of methyl vinyl ketone oxide: A four-carbon unsaturated Criegee intermediate from isoprene ozonolysis. *J. Chem. Phys.* **2021**, *155*, 174305. [CrossRef]
27. McCoy, J.C.; Marchetti, B.; Thodika, M.; Karsili, T.N.V. A Simple and Efficient Method for Simulating the Electronic Absorption Spectra of Criegee Intermediates: Benchmarking on CH_2OO and CH_3CHOO. *J. Phys. Chem. A* **2021**, *125*, 4089–4097. [CrossRef]
28. Esposito, V.J.; Liu, T.; Wang, G.; Caracciolo, A.; Vansco, M.F.; Marchetti, B.; Karsili, T.N.V.; Lester, M.I. Photodissociation Dynamics of CH2OO on Multiple Potential Energy Surfaces: Experiment and Theory. *J. Phys. Chem. A* **2021**, *125*, 6571–6579. [CrossRef]
29. Antwi, E.; Bush, R.; Marchetti, B.; Karsili, T. A Direct Dynamics Study of the Exotic Photochemistry of the Simplest Criegee Intermediate, CH_2OO. *Phys. Chem. Chem. Phys.* **2022**, *24*, 16724–16731. [CrossRef]
30. Antwi, E.; Ratliff, J.M.; Ashfold, M.N.R.; Karsili, T.N.V. Comparing the Excited State Dynamics of CH_2OO, the Simplest Criegee Intermediate, Following Vertical versus Adiabatic Excitation. *J. Phys. Chem. A* **2022**, *126*, 6236–6243. [CrossRef]

31. Antwi, E.; Packer, N.A.; Ratliff, J.M.; Marchetti, B.; Karsili, T.N.V. Insights into the Ultrafast Photodissociation Dynamics of Isoprene Derived Criegee Intermediates. *Photochem. Photobiol.* **2022**, *99*, 1072–1079. [CrossRef]
32. Wang, G.; Liu, T.; Zou, M.; Sojdak, C.A.; Kozlowski, M.C.; Karsili, T.N.V.; Lester, M.I. Electronic Spectroscopy and Dissociation Dynamics of Vinyl-Substituted Criegee Intermediates: 2-Butenal Oxide and Comparison with Methyl Vinyl Ketone Oxide and Methacrolein Oxide Isomers. *J. Phys. Chem. A* **2023**, *127*, 203–215. [CrossRef]
33. Butcher, J.C. A Modified Multistep Method for the Numerical Integration of Ordinary Differential Equations. *J. ACM* **1965**, *12*, 124–135. [CrossRef]
34. Park, J.W.; Shiozaki, T. Analytical Derivative Coupling for Multistate CASPT2 Theory. *J. Chem. Theory Comput.* **2017**, *13*, 2561–2570. [CrossRef] [PubMed]
35. Shiozaki, T. BAGEL: Brilliantly Advanced General Electronic-structure Library. *Wiley Interdiscip. Rev. Comput. Mol. Sci.* **2018**, *8*, e1331. [CrossRef]
36. Fang, Y.; Liu, F.; Barber, V.P.; Klippenstein, S.J.; McCoy, A.B.; Lester, M.I. Communication: Real time observation of unimolecular decay of Criegee intermediates to OH radical products. *J. Chem. Phys.* **2016**, *144*, 61102. [CrossRef]
37. Esposito, V.J.; Werba, O.; Bush, S.A.; Marchetti, B.; Karsili, T.N.V. Insights into the Ultrafast Dynamics of CH_2OO and CH_3CHOO Following Excitation to the Bright $1\pi\pi^*$ State: The Role of Singlet and Triplet States. *Photochem. Photobiol.* **2021**, *98*, 763–772. [CrossRef]